Sustainable Carbon-Based Biosorbent Particles from Papaya Seed Waste: Preparation and Adsorption isotherm

R. Ragadhita[1], A. Amalliya[1], S. Nuryandi[1], M. Fiandini[1], A. B. D. Nandiyanto[1,2*], A. Hufad[1], A. Mudzakir[1], W. C. Nugraha[2], O. Farobie[3], I. Istadi[4], A.S.M. Al-Obaidi[5]

[1]Universitas Pendidikan Indonesia, Jl. Setiabudhi No. 229, Bandung, Indonesia
[2]Research Unit for Clean Technology, National Research and Innovation Agency, Cisitu, Bandung, Indonesia
[3]IPB University, Jl. Padjajaran No.1, Bogor, Indonesia
[4]Department of Chemical Engineering, Universitas Diponegoro, Semarang, Indonesia
[5]School of Computer Science and Engineering, Taylor's University, Subang Jaya, Selangor, Malaysia
*Corresponding author, Email address: nandiyanto@upi.edu

Abstract: In the sustainability paradigm, the concept of converting waste into valuable products is one of the problem solvers. The goal of this study was to investigate the adsorption mechanism of carbon-based adsorbent particles from papaya seed waste with various sizes (i.e. 500, 1000, and 2000 microns) that can be used as alternative adsorbents in pollutant removal in aqueous solution. In the experiment, papaya seeds were carbonized at 400°C for 4 hours and ground to produce carbon-based particles, which were then used as adsorbent. The adsorption characteristics of curcumin (as a dye model) by carbon adsorbents were evaluated in a batch reactor. The results showed that adsorption occurred via monolayer (for small adsorbents) and multilayer (for large adsorbents). Concerns on the size of the adsorbent have been found, playing a role in the enhancement of adsorption capacity due to its offering the existence of a larger surface area. In addition, small adsorbents have attractive electrostatic adsorbent-adsorbate interaction, giving benefits in the adsorption process, while large adsorbents have issues in the repulsive electrostatic interaction. In conclusion, effective carbon-based adsorbents can be designed and produced from papaya stem wastes, providing alternative ways to remove pollutants from aqueous solutions, thereby achieving the primary objective of the sustainable development goals (SDGs).

Keywords: Adsorption, Carbon microparticles, Adsorption isotherm, Papaya seed, Particle size, Sustainable development goals (SDGs).

1. Introduction

A healthy environment is required for the achievement of Sustainable Development Goals (SDGs) (Tapia-Orozco *et al.*, 2004; Mirzaei *et al.,* 2016; Ojediran *et al.,* 2021). SDG 6 prescribes access to safe water and sanitation, as well as sound management of freshwater ecosystems, which are critical to human health, environmental sustainability, and economic prosperity (Unuabonah *et al.*, 2019). If this goal is not met, it could have serious consequences for the survival of life on earth. As a result, water is critical to the survival of humans, flora, and fauna. It is a valuable resource for global advancement, civilization, and industrialization, which has resulted in an improvement in the standard of living. The global water demand is increasing daily, owing to the world's growing population and increased

industrialization in many countries (Onda *et al.*, 2012). In the past, heavy metal pollution (Joseph *et al.*, 2019), dyes (Yagub *et al.*, 2014; Hassan *et al*., 2022; Akartasse *et al.,* 2022), pesticides (de Souza *et al.*, 2020), pharmaceuticals (Lima, 2018), radioactive elements (Zhang *et al.*, 2019), phenol derivative compounds (Ahmaruzzaman, 2008; Jodeh *et al.* 2014), and other emerging contaminants have all been linked to water pollution. To ensure an adequate supply of water, the management of water resources is important. Water treatment is a system for treating low-quality water to achieve the desired or predetermined quality of water. Because clean water is one of humanity's most basic needs, it will be used following the desired results (Saleh, 2021).

The methods used to treat wastewater to avoid pollution can be broadly classified into four types: physical and chemical processes, biological processes, radioactive methods, and electrical methods (Karimi-Maleh *et al.*, 2021; Pavithra *et al.*, 2019; Bouknana *et al.* 2014). There are various wastewater treatment methodologies, such as membrane technology, which is used to regulate specific contaminants (Rathi *et al.*, 2021). Emerging contaminants, a class of toxins in the atmosphere with low intensity but high toxicity, have received a lot of attention recently. Such trace contaminants could accumulate in species and be transmitted to living organisms, posing a public health risk (Rout *et al.*, 2021). Biochar, a low-cost and high-efficiency adsorbent, was used to combat emerging toxins in the water. However, adsorption mechanisms are typically non-specific and could be used to eliminate or reduce a wide range of contaminants (Gupta *et al.*, 2009). Adsorption is a well-known surface phenomenon that also serves as a method for equilibrium separation and an efficient method for removing contaminants from wastewater (Ragadhita and Nandiyanto, 2021). Adsorption was found to be superior to other wastewater treatment methods in terms of initial cost, simplicity of design, ease of use, and resistance to harmful substances (Kumar *et al.*, 2019). As a result, adsorption prevents the formation of hazardous chemicals. Carbon particle is now the most widely used adsorbent. This is widely used to remove complex contaminants from wastewater, such as dyes and heavy metals (Prasannamedha *et al.*, 2021). In more detail, a summary of the research on carbon-based adsorbents for wastewater treatment is presented in **Table 1**. As mentioned before, a variety of low-cost adsorbents were evaluated for their ability to remove various types of contaminants from wastewater. Papaya seeds are widely used as biosorbent of various dyies and heavy metals (Foleto *et al.*, 2012; Rangabhashiyam *et al.*, 2018; Nipa *et al.*, 2023). Nipa *et al.* (2023) found that a higher correlation coefficient, the rate of sorption was shown to match the pseudo–second–order kinetic model with reundlich isotherm model have better fit than Langmuir isotherm model. The kinetic results of removal of methylene Blue on activated carbon/chitosan/Carica papaya seeds were best fitted to the pseudo-second-order and Elovich models (Idohou *et al.*, 2020).

The current research addresses the source of contaminants as well as the concept of adsorption in the separation of emerging contaminants. The main goal of this work was to investigate the adsorption mechanism of carbon-based adsorbent particles from papaya seed waste with various sizes (i.e. 500, 1000, and 2000 microns) that can be used as alternative adsorbents in pollutant removal in aqueous solution.

2.   Adsorption theory

A brief overview of ten adsorption isotherms was examined to analyze the adsorption mechanism and the calculation for gaining the curves from data fitting results are presented in **Table 2**. Detailed calculation on adsorption isotherm is explained in previous literature (Ragadhita and Nandiyanto, 2021).

Table 1. Research summary about the application of carbon-based material for wastewater treatment

No	Source of Carbon	Results	Ref.
1	Rice Husk	The rice husk that has been prepared is agglomerated even though the size of 800 nm is obtained. but it has the efficiency to be used as an adsorbent.	(Fiandini *et al.,* 2020)
2	Oil Palm Shell	The results of this study stated that optimal absorption occurred at a concentration of 10 ppm, with a time of 40 minutes and a pH of 3-4. Heavy metals Cd and Pb absorbed reached 84.61-80.13%.	(Gultom and Lubis, 2014)
3	Corn Stalks Fiber	The results of this study indicate that corn stalks fiber can absorb methylene blue with an absorption capacity of rhodamine B of 7.81 mg/g and a correlation coefficient (R^2) of 0.974, while the absorption capacity of methylene blue is 9.09 mg/g with a correlation coefficient (R^2) of 0.963.	(Wulandary, 2019)
4	Cassava Peel	Cassava peel carbon can work in reducing impurities and heavy metals found in wells so that the specifications produced are following the requirements for clean water quality.	(Maulinda *et al*., 2017)
5	Coffee Grounds	The absorption of color from coffee grounds by processed coffee powder activated carbon and used as an adsorbent complies with the Freundlich equation and a K_f value of 0.021 is obtained.	(Fernianti, 2013)
6	Pineapple Peel	The highest effectiveness of pineapple peel as an adsorbent is when adding 125μm of pineapple peel waste mass with an absorption efficiency of 94.45%.	(Nandiyanto *et al*., 2020b)
7	Ngapi Nut Peel	The results of this study showed that the best adsorption of Cd(II) metal ions was obtained at the adsorbent mass of 1 g/50 mL of liquid waste with an absorption capacity of 1.32 mg/g.	(Pandia and Warman, 2016)
8	Kluwak Peel	The results showed that the greatest efficiency of phenol removal with kluwak shell carbon occurred at a carbon dose of 1.5 grams, namely 19.9%.	(Arif *et al*., 2015)
9	Durian Seed	The results of the study explained that durian seeds can absorb methyl blue at pH 3 with an efficiency value of 99.62%.	(Moelyaningrum *et al*., 2018)
10	Siamese Orange Peel	The results of the study explained that Siamese orange peel can absorb Pb(II) metal at pH 4.0 with an absorption percentage of 97.48% and an absorption capacity of 4.947 mg/g.	(Solika *et al*., 2018)
11	Jackfruit Peel	The results of the study explained that jackfruit skin can absorb Rhodamine B with an absorption capacity of 14.20 mg/g.	(Sunarsih and Dahani, 2018)
12	Avocado Seeds	The results of the study explained that avocado seeds can absorb Pb metal with fairly good efficiency due to the presence of tannins	(Kristianto *et al.,* 2018)

Table 2. A brief overview of ten adsorption isotherm models

Isotherm Model	Theoretical Consideration	Plot (x-axis vs y-axis)	Parameter
Langmuir	The model assumes monolayer adsorption, where adsorbates are adsorbed to a finite number of identical and equivalent definite localized sites with no lateral interaction, supported using **Eqn. 1**: $$\frac{1}{Qe} = \frac{1}{Qmax^{Kl}}\frac{1}{C_e} + \frac{1}{Qmax}$$ **Eqn. 1** Where K_L is the Langmuir constant, qe is the number of molecules adsorbed at equilibrium (mg/g), and qm is the adsorption capacity (mg/g). The adsorption factor (R_L) is expressed by **Eqn. 2:** $$R_L = \frac{1}{1+K_LC_e}$$ **Eqn.2** R_L describes conditions: unfavorable adsorption ($R_L > 1$); linear adsorption (affected by the amount and concentration of adsorbed molecules) ($R_L = 1$); too strong adsorption or irreversible adsorption ($R_L = 0$); and favorable adsorption or no desorption ($0 < R_L < 1$).	$\frac{1}{C_e}$ vs $\frac{1}{Q_e}$	• $\frac{1}{Q_{max}} = intercept$ • $K_L = \frac{1}{Q_{max}\times slope}$
Freundlich	The model describes multilayer adsorption on heterogeneous surfaces caused by differences in adsorption heat, represented by **Eqn. 3**: $$log\,Q_e = logk_f + \frac{1}{n}log\,C_e$$ **Eqn.3** Where k_f is the Freundlich constant that estimates the adsorption capacity and Ce is the adsorbate concentration at equilibrium (mg/L). n is the degree of nonlinearity and the adsorption strength, following chemisorption ($n < 1$) or physisorption ($n > 1$); linear adsorption (a concentration-independent partition between two phases) (n = 1); normal adsorption ($1/n < 1$); cooperative adsorption ($1/n > 1$); favorable adsorption or no desorption ($1 < 1/n < 0$); and adsorption on a heterogeneous surface ($0 < 1/n < 1$; the closer to zero indicates increasing heterogeneous adsorbent surface).	lnC_e vs lnQ_e	• $lnK_F = intercept$ • $\frac{1}{n} = slope$
Temkin	This model concerns interactions between adsorbent and adsorbate, assuming that the heat of adsorption of molecules decreases linearly in each adsorbed layer and excludes high and low concentration values, represented by **Eqn. 4**: $$q_e = B_TlnA_T + B_TlnC_e$$ **Eqn.4** where AT is the equilibrium constant of the Temkin model. βT is the Temkin constant, informing physical ($\beta_T < 8$ kJ) or chemical ($\beta_T > 8$ kJ) adsorption.	lnC_e vs Q_e	• $B = slope$ • $B_TlnA_T = intercept$ • $B_T = \frac{RT}{B}$
Dubini-Radushkevich	This model is based on the adsorption of gases by porous adsorbents and the pore-filling mechanism, represented by **Eqn. 5:** $$lnq_e = lnq_s - (\beta\varepsilon^2)q_e$$ **Eqn. 5**	ε^2 vs lnQ_e	• $\beta = K_{DR} = slope$ • $E = \frac{1}{\sqrt{2\times K_{DR}}}$

Where q_s is the saturation capacity (mg/g) and β is the Dubinin-Radushkevich constant correlating to the average free adsorption energy. ε is the Polanyi potential associated with equilibrium conditions, in which the value correlates to adsorption energy (E) (see **Eqn. 6** and **7**:

$$\varepsilon = RTln\left[1 + \frac{1}{C_e}\right] \qquad \textbf{Eqn. 6}$$

$$E = \frac{1}{\sqrt{2\beta}} \qquad \textbf{Eqn. 7}$$

E relates to the physical ($E < 8$ kJ) or chemical ($E > 8$ kJ) adsorption

---

Flory-Huggins

This model is based on the adsorption of gases by porous adsorbents and the pore-filling mechanism, represented by **Eqn. 8:**

$$log\frac{\theta}{Ce} = logK_{FH} + n\,log\,log(1-\theta) \quad \textbf{Eqn. 8}$$

Where $\theta = \left(1 - \frac{C_e}{C_o}\right)$ is the degree of monolayer coverage. n_{FH} and K_{FH} are the equilibrium constant for the Flory-Huggins model, in which it correlates to the Gibbs free energy ($\Delta G°$), as presented in **Eqn. 9:**

$$\Delta G° = -RT\,ln\,K_{FH} \qquad \textbf{Eqn. 9}$$

The $\Delta G°$ can describe the spontaneous and temperature-dependent nature of the adsorption when it is negative.

$log\left(\frac{\theta}{C_0}\right)$ vs $log(1-\theta)$

- $n_{FH} = slope$
- $k_{FH} = intercept$
- $\Delta G^{\underline{o}} = RTln(k_{FH})$
- $\theta = 1 - \left(\frac{C_e}{C_0}\right)$

Fowler-Guggenheim

This model is based on the adsorption of gases by porous adsorbents and the pore-filling mechanism, represented by **Eqn. 10:**

$$K_{FG}C_e = \frac{\theta}{1-\theta}exp\left(\frac{2.\theta.W}{RT}\right) \qquad \textbf{Eqn. 10}$$

W is the interaction energy between the adsorbed molecules (kJ/mol), informing processes under exothermic ($W > 0$), endothermic ($W < 0$ kJ/mol), or no interaction between adsorbed molecules ($W = 0$ kJ/mol).

vs $ln\left[\frac{C_e(1-\theta)}{\theta}\right]\theta$

- $W = slope$
- $-lnK_{FG} = intercept$
- $\alpha\,(slope) = \frac{2W\theta}{RT}$
- $\theta = 1 - \left(\frac{C_e}{C_0}\right)$

Hill Deboer

This model is based on the adsorption of gases by porous adsorbents and the pore-filling mechanism, represented by **Eqn. 11:**

$$K_1.C_e = \frac{\theta}{1-\theta}exp\left(\frac{\theta}{1-\theta} - \frac{K_2\theta}{RT}\right) \qquad \textbf{Eqn. 11}$$

Where K_1 (L/mg) and K_2 (kJ/mol) are the contact energy constants for the adsorbed molecules, K2 informing: exothermic with intermolecular adsorption ($K_2 > 0$); endothermic with repulsion ($K_2 < 0$), or no interaction between adsorbates ($K_2 = 0$).

θ vs $ln\left[\frac{C_e(1-\theta)}{\theta}\right] - \frac{\theta}{1-\theta}$

- $-lnk_1 = intercept$
- $\alpha\,(slope) = \frac{k_2\theta}{RT}$
- $\theta = 1 - \left(\frac{C_e}{C_0}\right)$

Jovanovic

The model evaluates adsorption on a heterogeneous surface where a multilayer form during the adsorption, represented in **Eqn. 12:**

$$lnQ_e = lnQ_{max} - K_jC_e \qquad \textbf{Eqn. 12}$$

Where Q_e is the amount of adsorbate in the adsorbent at equilibrium (mg/g), Q_{max} is the maximum absorption of the adsorbate, and K_J is

C_e vs lnQ_e

- $K_J = slope$
- $lnq_{max} = intercept$

---

	the Jovanovic constant. At a high concentration of adsorbate, the preceding equation becomes the Langmuir isotherm.		
Harkin-Jura	The model evaluates adsorption on a heterogeneous surface where a multilayer form during the adsorption, represented in **Eqn. 13:** $$\frac{1}{q_e^2} = \frac{B_{HJ}}{A_{HJ}} - \left(\frac{1}{A}\right) logC_e \qquad \textbf{Eqn. 13}$$ B_{HJ} is related to the specific surface area of the adsorbent and A_{HJ} is the Harkin-Jura constant.	$logC_e$ vs $\frac{1}{q_e^2}$	• $A_H = \frac{1}{Slope}$ • $\frac{B_H}{A_H} = intercept$
Halsey	This model evaluates the multilayer adsorption system at a relatively large distance from the surface. Similarly to the Freundlich model, the Halsey model applies to both multilayer adsorption and heterogeneous surfaces with non-uniformly distributed adsorption heat, represented in **Eqn. 14:** $$Q_e = \frac{1}{n_H} lnK_H - \left(\frac{1}{n_H}\right) lnC_e \qquad \textbf{Eqn. 14}$$ where K_H and n are Halsey's constants	lnC_e vs lnQ_e	• $\frac{1}{n} = slope$ • $\frac{1}{n} lnK_H = intercept$

3. Material and Method

3.1 Adsorbent-based carbon particle preparation

In this study, papaya seeds were used as raw material for carbon-based adsorbents. To fabricate carbon adsorbent, papaya seeds were cut into small pieces, cleaned, and carbonized at 250°C for 5 hours in an electric furnace. To obtain a homogeneous particle size of papaya seed-based carbon, carbon from papaya seeds was ground. After that, a sieving test (Yayasan Bumi Publikasi Nusantara, Indonesia; sizes of 2000, 1000, 500, 250, 125, 99, and 74 µm) was carried out to obtain a specific particle size.

3.2 Adsorbent characterization

To analyze the carbon particles that have been successfully fabricated, particle morphology analysis was carried out with a Digital Microscope (BXAW-AX-BC, China). Analysis of the functional group of the prepared carbon was performed using Fourier Transform Infrared (FTIR-4600, Jasco Corp., Japan).

3.3 Adsorption experimental process

Curcumin in aqueous solutions (concentrations of 20, 40, 60, 80, and 100 ppm) was mixed with 0.5 g of the prepared carbon particles (specific sizes of 2000, 1000, and 500 m) for 24 hours in the adsorption experiment (a glass batch reactor with a total volume of 1 L) (in the dark condition). Blank solutions (curcumin solutions without additional carbon) were also tested under the same process conditions and served as a standard comparison. During the adsorption, an aliquot sample (3 mL) was taken at specific hours and tested using a visible spectrophotometer (Model 7205 JENWAY; Cole-Parmer; US), and the measurement curve results were normalized and entered into the Lambert-Beer formula to determine the actual concentration at that time. During the adsorption process, variations in the size of the adsorbent particles were tested to determine the effect of the adsorbent particle size on the absorption of curcumin. Adsorption systems using sizes of 500, 1000, and 2000 µm are labeled as small particle size (SP), medium particle size (MP), and large particle size (LP), respectively.

4. Results and Discussion

4.1 Characterization of adsorbent-based carbon particle

Figure 1(a) shows the results of the surface structure of carbon microparticles from papaya seeds. In **Figure 1(a)**, the physical form of carbon particles is black with irregular shapes. **Figure 1(b)** represents the results of ferret analysis of the particle size distribution of carbon from papaya seeds. In general, the carbon particles used have a size between 100-500 μm with an average particle size of 700 μm. **Figure 1(c)** is the result of the FTIR analysis of carbon particles from papaya seeds. FTIR results in **Figure 1(c)**, all sizes of carbon have identical wavelengths. As shown in **Figure 1(c)**, all particles have several functional groups at wavelengths including hydroxyl groups (-OH) at 3848-3589 cm^{-1}, aliphatic compounds at 2854-3859 cm^{-1}, carbonyl compounds (C=O) at 1617-1817 cm^{-1}, the C-H group stretches at wave 1300-1400 cm^{-1}, the vibrational stretching of C-O at a wavelength of 1023-1200 cm^{-1} (Kristianto *et al.,* 2018; Zhang *et al*., 2019; Nandiyanto *et al.,* 2019).
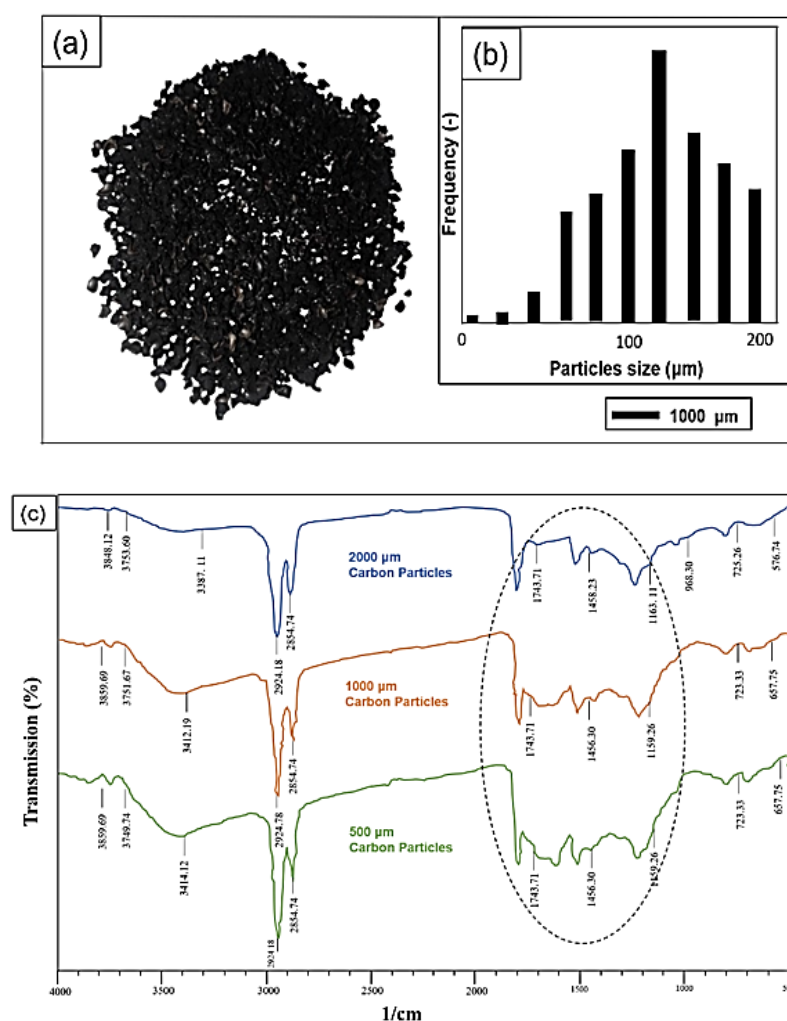

Figure 1. Microscope images of carbon particles (a) with their size distribution (b). Figure (c) is the FTIR analysis results of carbon with different sizes.

4.2 Adsorption Isotherm

Adsorption isotherm analysis is a critical step in determining the best adsorption equilibrium correlation to quantitatively predict the parameters and characteristics of how a pollutant interacts with a specific adsorbent to optimize the adsorption pathway mechanism, expression of surface properties, and adsorbent capacity. Adsorption isotherms are evaluated and achieved here by comparing

adsorption results and adsorption isotherm models (see **Table 3**). Detailed proposed adsorption mechanism based on the adsorption isotherm model is illustrated in **Figures 2(a)** and **(b)**.

The Langmuir model assumes that an adsorbate monolayer covers the adsorbent surface with no interaction between adsorbed molecules. Adsorption in heterogeneous systems is commonly described using the Freundlich model (Xia *et al.*, 2021). From the Langmuir isotherm, carbon adsorbent particles based on papaya seeds with particle sizes of SP, MP, and LP have maximum adsorption capacities of 370.350; 344.82; and 232.558 mg/g, respectively. The Langmuir model's binding energy constant (K_L) is calculated for an adsorption system labeled SP > MP > LP, where K_L measures the adsorbate's affinity for the adsorbent. A high K_L value indicates that the adsorbate and adsorbent surface has a strong attraction (Turp *et al.*, 2020). The K_f constant obtained from the Freundlich isotherm indicates adsorption capacity, whereas n indicates the adsorption process's favorability. The resulting K_f values for different particle sizes are SP > MP > LP, which is consistent with the Langmuir isotherm results. All of the adsorption systems have n values between 1 and 10, indicating a favorable adsorption process (Ayawei *et al.*, 2017).

The Temkin model takes into account the indirect adsorbate interaction effect and assumes that the heat of adsorption decreases linearly with coverage. All of the studied adsorption processes had b_T values smaller than 8 kJ/mol, indicating weak interactions between the adsorbate and adsorbent (Sarma *et al.*, 2019). Dubinin-Radushkevich isotherm expresses the adsorption mechanism with a Gaussian energy distribution onto a heterogeneous surface and is commonly used to distinguish between physical and chemical metal ion adsorption by observing the mean free energy value (E). Adsorption energy is commonly used to differentiate between physical and chemical adsorption. Adsorption energy is typically less than 8 kJ/mol for physical adsorption mechanisms and 8 kJ/mol to 16 kJ/mol for chemical adsorption mechanisms (El Maguana *et al.*, 2020). The adsorption energy values for all of the adsorption studied range from 1.4 kJ/mol to 2.0 kJ/mol, indicating a physical adsorption mechanism.

The Flory Huggins isotherm describes the formation of multilayers of adsorbate molecules on the surface of the biosorbent when the n_{FH} parameter is greater than one, and the molecule will be involved in more than one active site when the n_{FH} parameter is less than one. Although the Flory-Huggins model has a significant R^2 value, the value of the n_{FH} parameter obtained in this model is negative, which is practically impossible for an adsorption system using MP and LP (Nayak and Pal, 2020; Ahmadou *et al.*, 2023). As a result, no explanation using this isotherm model is valid. Furthermore, the K_{FH} equilibrium constant obtained from the Flory-Huggins isotherm equation is used to investigate the Gibbs free energy ($\Delta G°$) of spontaneity. The $\Delta G°$ values for curcumin adsorption were found to be negative in all adsorption systems studied, indicating a spontaneous adsorption property (Tsamo *et al.*, 2020).

The Fowler-Guggenheim isotherm describes the lateral interactions between the adsorbent and the adsorbed molecule (Nandiyanto, 2020a; Salahat et al., 2023). When W is negative, the interaction equation for adsorbate molecules is represented by attraction, and when W is positive, it is represented by repulsion. However, if there is no interaction between the adsorbed molecules, $W = 0$ (Nayak and Pal, 2020). A negative W value indicates that the adsorbed molecules have an attractive interaction. In this case, the attractive interactions increase as particle size decreases, favoring the possibility of lateral interactions between adsorbed molecules.

In a dynamic adsorption system, the Hill-de Boer isotherm represents the lateral interaction between adsorbed molecules. The K_2 value represents the interaction between adsorbed molecules. Table 3 shows that the coefficient of interactions (K_2) was found to be negative for all adsorption systems, confirming the presence of repulsive forces between adsorbed and adsorbent molecules

(Nayak and Pal, 2020). As a result, the monolayer phenomenon can be predicted using repulsive interactions between adsorbed molecules. Table 3 also shows that the value of K_2 increases as particle size decreases, indicating that adsorption is more beneficial at smaller particle sizes (Nayak and Pal, 2020). The Jovanovic isotherm shows a good agreement with the Langmuir isotherm, in which particles with small sizes have the maximum adsorption capacity. The adsorption capacities for the SP > MP > LP > adsorbent systems were 138.074; 82.44; and 4.9599 mg/g, respectively.

The Harkins-Jura model assumes multilayer adsorption on surface adsorbents with heterogeneous pore distribution (Ragadhita and Nandiyanto, 2021). The Harkin Jura model, like the Halsey model, describes multilayer adsorption at relatively great distances from the surface and with the heterogeneous adsorbent (Ragadhita and Nandiyanto, 2021). The correlation coefficient (R^2) values for all adsorption systems demonstrated a good fit with the two models, demonstrating the suitability of curcumin adsorption with this model principle. Compatibility with these two models confirms compatibility with the Freundlich isotherm model.

Table 3. Detailed data of adsorption isotherm parameters

Model	Parameter	Particle Size (µm)			Note
		2000	1000	500	
Freundlich	R^2	0.80902	0.9949	0.86616	$R^2 < 0.70$, monolayer formation on the adsorbent surface $R^2 > 0.70$, multilayer formation on the adsorbent surface
	K_f	1.2431	1.4841	7.4359	Freundlich constant of adsorption isotherm
	n	1.1477	2.5325	4.5944	Physisorption process ($n > 1$)
	$1/n$	0.2176	0.3948	0.8713	Favorable cooperative adsorption
Langmuir	R^2	0.84038	0.99825	0.80902	$R^2 > 0.70$, monolayer formation on the adsorbent surface $R^2 < 0.70$, multilayer formation on the adsorbent surface
	Q_{max}	232.558	344.82	370.370	Maximum capacity of adsorbent (mg/g)
	R_L	0.0030	0.0062	0.0769	Favorable adsorption ($0 < 1/n < 1$)
	K_L	0.00823	0.055	0.1310	Constants Langmuir model
Temkin	R^2	0.867335	0.99825	0.86734	Monolayer ($R^2 > 0.70$) on the adsorbent surface.
	A_T (L/g)	1.4986	1.9428	6.947	Binding constant for the Temkin equilibrium
	β_T (J/mol)	0.6055	0.3057	0.1607	Physical process adsorption ($\beta_T > 8$ kJ/mol)

Dubinin-Radushkevich	R^2	0.70934	0.96551	0.92123	$R^2 < 0.70$, homogenous adsorbent surface $R^2 > 0.70$, heterogenous adsorbent surface
	Qs (mg/g)	1.545	1.254	1.350	Adsorbent's capacity for adsorption
	β (mol²/kJ²)	0.1262	0.2138	0.2235	The Dubinin-Radushkevich constant
	E (kJ/mol)	1.4957	1.529	1.992	Physical interaction between adsorbate molecules
Flory Huggins	R^2	0.95251	0.99537	0.00054	-
	n_{FH}	-0.90281	-0.7187	0.0090	• Adsorbate is present in more than one active adsorbent zone ($n_{FH} < 1$) multilayer of adsorbate molecules formation ($n_{FH} > 1$)
	K_{FH} (L/mg)	6.261	186.208	406.069	Flory Huggins constant
	$\Delta G°$ (kJ/mol)	-134.46	-117.008	-41.06	• Spontaneous adsorption ($\Delta G° < 0$) • Non-spontaneous adsorption ($\Delta G° > 0$)
Fowler-Guggenheim	R^2	0.997437	0.99003	0.94322	$R^2 > 0.70$, monolayer formation on the adsorbent surface $R^2 < 0.70$, multilayer formation on the adsorbent surface
	K_{FG} (L/mg)	1.4090×10^{-5}	7.2102×10^{-7}	4.536×10^{-6}	Constants for the Fowler-Guggenheim model
	W (kJ/mol)	-15.4736	-13.2492	-11.9755	$W < 0$ kJ/mol, the interaction between adsorbed molecules will be attractive
Hill Deboer	R^2	0.98557	0.98309	0.39633	$R^2 > 0.70$, monolayer formation on the adsorbent surface $R^2 < 0.70$, multilayer formation on the adsorbent surface
	K_1 (L/mg)	2.824×10^{-9}	1.670×10^{-12}	1.894×10^{-19}	Constant for the Hill-Deboer model
	K_2 (L/mg)	-822.790	-1082.59	-1640.28	Repulsive interaction between adsorbed species

Jovanovic	R^2	0.963004	0.92964	0.71915	$R^2 > 0.70$, monolayer formation on the adsorbent surface $R^2 < 0.70$, multilayer formation on the adsorbent surface
	K_J (L/mg)	0.0064	0.0130	0.0469	Constants for the Jovanovic model
	Qmax (mg/g)	4.9599	82.44	138.074	Maximum capacity of adsorbent (mg/g)
	R^2	0.953119	0.950851	0.75153	$R^2 > 0.70$, multilayer formation on the adsorbent surface $R^2 < 0.70$, monolayer formation on the adsorbent surface
	A_{HJ}	0.035	0.027	0.086	Relates to the surface area of the adsorbent
	B_{HJ}	0.0000758	0.00009192	0.000206	Relates to the surface area of the adsorbent
	R^2	0.953119	0.950851	0.75153	$R^2 > 0.70$, multilayer formation on the adsorbent surface $R^2 < 0.70$, monolayer formation on the adsorbent surface
Halsey	R^2	0.900692	0.98705	0.80902	$R^2 > 0.70$, multilayer formation on the adsorbent surface $R^2 < 0.70$, monolayer formation on the adsorbent surface
	n	4.5943	2.5325	1.1476	Constants for the Halsey model
	K_H	85.223	54.996	15.873	Constants for the Halsey model
	R^2	0.900692	0.98705	0.80902	$R^2 > 0.70$, multilayer formation on the adsorbent surface $R^2 < 0.70$, monolayer formation on the adsorbent surface

The results of the suitability analysis based on the results of the R^2 fitting value, the adsorption of curcumin with various sizes of papaya seed-based carbon particles has the following compatibility:

(i) for an adsorbent with a small particle size (500 µm), the order of the suitable adsorption model is Fowler Guggenheim > Dubinin-Radushkevich > Freundlich. Meanwhile, for adsorbents that have a medium particle size (1000 µm), the order of suitability for the isotherm model is Temkin > Freundlich > Flory-Huggins. Models that match both types of particle sizes express that the adsorption process through the formation of multilayers, the spontaneous, favorable, attractive interaction between adsorbates and adsorbent, and also follows the pore-filling mechanism.

(ii) for adsorption using large particle sizes (2000 µm), the suitability of the model is Fowler Guggenheim > Hill Deboer > Jovanovic which shows that adsorption occurs by forming a monolayer,

physisorption, spontaneously, and follows pore-filling mechanism. However, the interaction between adsorbate and adsorbent is repulsive. Physisorption occurs as a result of weak electrostatic interactions such as London forces, dipole-dipole forces, and Van der Waals interactions, which cause the bands to be easily broken (Al-Ghouti and Da'ana, 2020). Here, the particle size sufficiently affects the adsorption capacity of papaya seed-based carbon adsorbents. The maximum adsorption capacity of the adsorbent increases significantly with decreasing particle size. This is because the smaller particle size has direct correlations to the promotion of a larger surface area, providing more sites for better adsorption ability (Wang and Shadman, 2013).
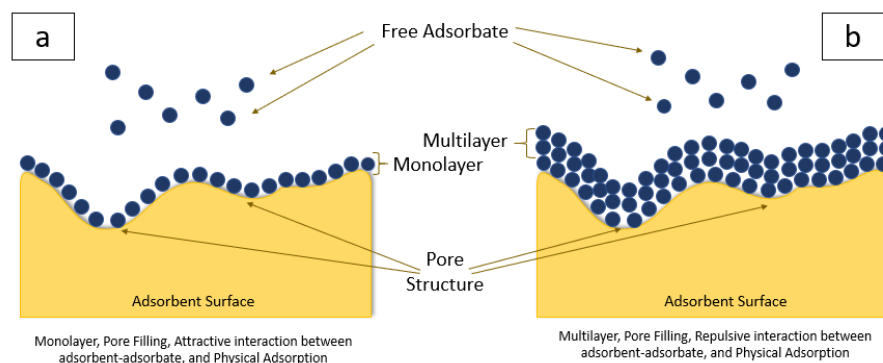

Figure 2. (**a**) Microscope images of carbon particles and (**b**) their size distribution (b). Figure (c) is the FTIR analysis results of carbon with different sizes.

Conclusion

Carbon material derived from papaya seeds was developed and used as an adsorbent for dye adsorption from aqueous solutions at low sorbate concentrations, which can support the need for a sustainable environment and clean water to help developing countries achieve the Sustainable Development Goals (SDGs). By analyzing the correlation coefficient, the equilibrium data were matched to 10 isotherm models, namely Langmuir, Freundlich, Temkin, Dubinin-Radushkevich, Flory Huggins, Fowler-Guggenheim, Hill Deboer, Jovanovic, Harkin Jura, and Halsey. For small adsorbents, adsorption occurs via the formation of monolayers (500 and 1000 µm). Adsorption occurs through the formation of multilayers at large adsorbent particle sizes (2000 µm). Adsorbents with small particle sizes (500 and 1000 µm) have attractive interaction characteristics based on adsorbent-adsorbate interaction, where these characteristics benefit the adsorption process. Adsorbent-adsorbate interaction is repulsive for a large adsorbent (2000 µm). According to the results, differences in the size of the adsorbent particles play a role, with the adsorption capacity increasing as the particle size decreases because the small particle size provides a larger surface area, resulting in a better adsorption process. According to the research findings, carbon-based products' good adsorption mechanism and low cost indicate that they can be used as effective adsorbents for water purification while protecting the environment.

Disclosure statement: *Conflict of Interest:* The authors declare that there are no conflicts of interest.
Compliance with Ethical Standards: This article does not contain any studies involving human or animal subjects

References

Ahmadou F., Abahdou F. Z., Slimani R., El Hajjaji S. (2023). Kinetic, isotherm and thermodynamic studies on the adsorption of Methylene blue dye using Moringa oleifera pods and kernels, *Mor. J. Chem.,* 14(1), 265-281. https://doi.org/10.48317/IMIST.PRSM/morjchem-v11i1.34864

Ahmaruzzaman M. (2008) Adsorption of phenolic compounds on low-cost adsorbents: a review. *Advances in Colloid and Interface Science*, 143(1-2), 48-67. doi.org/10.1016/j.cis.2008.07.002

Akartasse N., Azzaoui K., Mejdoubi E., Hammouti B., Elansari L.L., Abou-salama M., Aaddouz M., Sabbahi R., Rhazi L. and Siaj M. (2022). Environmental-Friendly Adsorbent Composite Based on Hydroxyapatite/Hydroxypropyl Methyl-Cellulose for Removal of Cationic Dyes from an Aqueous Solution, *Polymers,* 14(11), 2147; https://doi.org/10.3390/polym14112147

Al-Ghouti M.A., Da'ana D.A. (2020) Guidelines for the use and interpretation of adsorption isotherm models: A review. *J. hazard. Mater.*, 393, 122383. https://doi.org/10.1016/j.jhazmat.2020.122383

Arif A.R., Saleh A., Saokani J. (2015) Adsorpsi karbon aktif dari tempurung kluwak (Pangium edule) terhadap penurunan fenol. *Al-Kimia,* 3(1), 34-47.

Ayawei N., Ebelegi A.N., Wankasi D. (2017) Modelling and interpretation of adsorption isotherms. *Journal of chemistry*, https://doi.org/10.1155/2017/3039817.

Bouknana D., Hammouti B., Salghi R., Jodeh S., Zarrouk A., Warad I., Aouniti A., Sbaa M. (2014). Physicochemical Characterization of Olive Oil Mill Wastewaters in the eastern region of Morocco, *J. Mater. Environ. Sci.* 5 (4), 1039-1058

de Souza R.M., Seibert D., Quesada H.B., de Jesus Bassetti F., Fagundes-Klen M.R., and Bergamasco R. (2020) Occurrence, impacts and general aspects of pesticides in surface water: A review. *Process Safety and Environmental Protection*, 135, 22-37. https://doi.org/10.1016/j.psep.2019.12.035.

El Maguana Y., Elhadiri N., Benchanaa M., Chikri R. (2020) Activated carbon for dyes removal: modeling and understanding the adsorption process. *Journal of Chemistry*, 2020, 1-9. https://doi.org/10.1155/2020/2096834.

Fernianti D. (2013) Analisis kemampuan adsorpsi karbon aktif dari ampas kopi bubuk yang sudah diseduh. *Berkala Teknik*, 3(2), 563-572.

Fiandini M., Ragadhita, R., Nandiyanto, A.B.D., Nugraha, W.C. (2020) Adsorption characteristics of submicron porous carbon particles prepared from rice husk. *J. Eng. Sci. Technol*, 15, 022-031.

Foletto E.L., Weber C.T., Bertuol D. A.& Mazutti M.A. (2013) Application of Papaya Seeds as a Macro-/Mesoporous Biosorbent for the Removal of Large Pollutant Molecule from Aqueous Solution: Equilibrium, Kinetic, and Mechanism Studies, *Separation Science and Technology*, 48:18, 2817-2824, DOI: 10.1080/01496395.2013.808213

Gultom E.M., Lubis M.T. (2014). Aplikasi karbon aktif dari cangkang kelapa sawit dengan aktivator H_3PO_4 untuk penyerapan logam berat Cd dan Pb. *Jurnal Teknik Kimia USU*, 3(1), 5-10.

Gupta V.K., Carrott, P.J.M., Ribeiro Carrott, M.M.L., Suhas. (2009). Low-cost adsorbents: Growing approach to wastewater treatment—a review. *Critical Reviews in Environmental Science and Technology*, 39(10), 783-842. https://doi.org/10.1080/10643380801977610.

Hassan N., Shahat A., El-Didamony A., El-Desouky M.G., El-Bindary A.A. (2020), Equilibrium, Kinetic and Thermodynamic studies of adsorption of cationic dyes from aqueous solution using ZIF-8, *Mor. J. Chem.* 8, 627-63, https://doi.org/10.48317/IMIST.PRSM/morjchem-v8i3.21127

Jodeh S., Basalat N., Abu Obaid A., Bouknana D., Hammouti B., Hadda T. B., Jodeh W., Warad I. (2014). Adsorption of some organic phenolic compounds using activated carbon from cypress products, *J. Chem. Pharmac. Res.,* 6 N°2, 713-723

Joseph L., Jun, B.M., Flora, J.R., Park, C.M., and Yoon, Y. (2019). Removal of heavy metals from water sources in the developing world using low-cost materials: A review. *Chemosphere*, 229, 142-159. https://doi.org/10.1016/j.chemosphere.2019.04.198.

Idohou E. A., Fatombi J. K., Osseni S. A., Agani I., Neumeyer D., Verelst M., Mauricot R., Aminou T. (2020), Preparation of activated carbon/chitosan/Carica papaya seeds composite for efficient adsorption of cationic dye from aqueous solution, *Surfaces and Interfaces,* 21, 100741, ISSN

2468-0230, https://doi.org/10.1016/j.surfin.2020.100741

Karimi-Maleh H., Ranjbari, S., Tanhaei, B., Ayati, A., Orooji, Y., Alizadeh, M., and Sen, F. (2021). Novel 1-butyl-3-methylimidazolium bromide impregnated chitosan hydrogel beads nanostructure as an efficient nanobio-adsorbent for cationic dye removal: Kinetic study. *Environmental Research*, 195, 110809. https://doi.org/10.1016/j.envres.2021.110809.

Kristianto H., Kurniawan, M.A., and Soetedjo, J.N. (2018). Utilization of papaya seeds as natural coagulant for synthetic textile coloring agent wastewater treatment. *Int. J. Adv. Sci. Eng. Inf. Technol,* 8, 2071-2077.

Kumar P.S., Joshiba, G.J., Femina, C.C., Varshini, P., Priyadharshini, S., Karthick, M.A., Jothirani, R. (2019). A critical review on recent developments in the low-cost adsorption of dyes from wastewater. *Desalin. Water Treat*, 172, 395-416. doi: 10.5004/dwt.2019.24613

Lima E.C. (2018). Removal of emerging contaminants from the environment by adsorption. *Ecotoxicology and Environmental Safety*, 150, 1-17. https://doi.org/10.1016/j.ecoenv.2017.12.026.

Maulinda L., Nasrul Z.A., Sari D.N. (2017). Pemanfaatan kulit singkong sebagai bahan baku karbon aktif. *Jurnal Teknologi Kimia Unimal*, 4(2), 11-19.

Mirzaei A.; Chen Z., Haghighat F., Yerushalmi L. (2016). Removal of pharmaceuticals and endocrine disrupting compounds from water by zinc oxide-based photocatalytic degradation: A review. *Sustainable Cities and Society*, 27, 407-418. https://doi.org/10.1016/j.scs.2016.08.004.

Moelyaningrum A.D., Zarkasi K., Ningrum P.T. (2018). Penggunaan arang aktif kulit durian (Durio Zibethinus Murr) Terhadap tingkat adsorpsi kromium (Cr^{6+}) pada limbah batik. *Efektor*, 5, 67-73

Nandiyanto A.B.D. (2020a). Isotherm Adsorption of Carbon Microparticles Prepared from Pumpkin (Cucurbita maxima) Seeds Using Two-Parameter Monolayer Adsorption Models and Equations, *Mor. J. Chem.* 8, 745-761, https://doi.org/10.48317/IMIST.PRSM/morjchem-v8i3.21636

Nandiyanto A.B.D., Girsang G.C.S., Maryanti R., Ragadhita R., Anggraeni S., Fauzi F.M., Al-Obaidi A.S.M. (2020b). Adsorption isotherm characteristics of carbon microparticles prepared from pineapple peel waste. *Communications in Science and Technology*, 5(1), 31-39. https://doi.org/10.21924/cst.5.1.2020.176.

Nandiyanto A.B.D., Oktiani R., Ragadhita R. (2019). How to read and interpret FTIR spectroscope of organic material. *Indonesian Journal of Science and Technology*, 4(1), 97-118. https://doi.org/10.17509/ijost.v4i1.15806.

Nayak A.K., Pal A. (2020). Utilization of lignocellulosic waste for acridine orange uptake: insights into multiparameter isotherms modeling with ANN-aimed formulation. *Journal of Environmental Engineering*, 146(9), 04020096.

Nipa S. T., Nawrin Rahman Shefa, Shahanaz Parvin, Most Afroza Khatun, Md Jahangir Alam, Sujan Chowdhury, M. Azizur R. Khan, Sk Md Ali Zaker Shawon, Biplob K. Biswas, Md Wasikur Rahman, Adsorption of methylene blue on papaya bark fiber: Equilibrium, isotherm and kinetic perspectives, Results in Engineering, Volume 17, 2023, 100857, ISSN 2590-1230, https://doi.org/10.1016/j.rineng.2022.100857

Ojediran J.O., Dada, A.O., Aniyi, S.O., David, R.O., Adewumi, A.D. (2021). Mechanism and isotherm modeling of effective adsorption of malachite green as endocrine disruptive dye using Acid Functionalized Maize Cob (AFMC). *Scientific Reports*, 11(1), 21498.

Onda K., LoBuglio J., Bartram J. (2012). Global access to safe water: accounting for water quality and the resulting impact on MDG progress. *International Journal of Environmental Research and*

Public Health, 9(3), 880-894.

Pandia S., Warman, B. (2016). Pemanfaatan kulit jengkol sebagai adsorben dalam penyerapan logam CD (II) pada limbah cair industri pelapisan logam. *Jurnal Teknik Kimia USU*, 5(4), 57-63.

Pavithra K.G., Kumar, P.S., Christopher, F.C., Saravanan, A. (2017). Removal of toxic Cr (VI) ions from tannery industrial wastewater using a newly designed three-phase three-dimensional electrode reactor. *Journal of Physics and Chemistry of Solids*, 110, 379-385. https://doi.org/10.1016/j.jpcs.2017.07.002.

Prasannamedha G., Kumar P.S., Mehala R., Sharumitha T.J., Surendhar D. (2021). Enhanced adsorptive removal of sulfamethoxazole from water using biochar derived from hydrothermal carbonization of sugarcane bagasse. *Journal of Hazardous Materials*, 407, 124825. https://doi.org/10.1016/j.jhazmat.2020.124825.

Ragadhita R., Nandiyanto, A.B.D. (2021). How to calculate adsorption isotherms of particles using two-parameter monolayer adsorption models and equations. *Indonesian Journal of Science and Technology*, 6(1), 205-234. https://doi.org/10.17509/ijost.v6i1.32354.

Rangabhashiyam S., Sujata Lata, Balasubramanian P. (2018). Biosorption characteristics of methylene blue and malachite green from simulated wastewater onto Carica papaya wood biosorbent, *Surfaces and Interfaces,* 10, 197-215, https://doi.org/10.1016/j.surfin.2017.09.011

Rathi B.S., Kumar, P.S., Ponprasath R., Rohan K., Jahnavi N. (2021). An effective separation of toxic arsenic from aquatic environment using electrochemical ion exchange process. *Journal of Hazardous Materials*, 412, 125240. https://doi.org/10.1016/j.jhazmat.2021.125240.

Rout P.R., Zhang T.C., Bhunia P., Surampalli R.Y. (2021). Treatment technologies for emerging contaminants in wastewater treatment plants: A review. *Science of the Total Environment*, 753, 141990. https://doi.org/10.1016/j.scitotenv.2020.141990.

Salahat A., Hamed O., Deghles A., Azzaoui K., Qrareya H., Assali M., Mansour W., Jodeh S., Hacıosmanoğlu G.G., Can Z.S., Hammouti B., Nandiyanto A.B.D., Ayerdi-Gotor A., Rhazi L. (2023). Olive Industry Solid Waste-Based Biosorbent: Synthesis and Application in Wastewater Purification. *Polymers*, 15, 797. https://doi.org/10.3390/polym15040797

Saleh T.A. (2021). Protocols for synthesis of nanomaterials, polymers, and green materials as adsorbents for water treatment technologies. *Environmental Technology & Innovation*, 24, 101821. https://doi.org/10.1016/j.eti.2021.101821.

Sarma G.K., Sen Gupta S., Bhattacharyya K.G. (2019). Removal of hazardous basic dyes from aqueous solution by adsorption onto kaolinite and acid-treated kaolinite: kinetics, isotherm and mechanistic study. *SN Applied Sciences*, 1, 1-15. doi:10.1007/s42452-019-0216-y.

Solika N., Napitupulu, M., Gonggo, S.T. (2018). Bioadsorpsi Pb (II) Menggunakan Kulit Jeruk Siam (Citrus Reticulata). *J. Akad. Kim*, 6(3), 160.

Sunarsih S., Dahani W. (2018). Studi adsorpsi karbon aktif limbah kulit buah nangka terhadap Rhodamin B. *Jurnal Teknologi,* 11(1), 46-53.

Tapia-Orozco N., Ibarra-Cabrera R., Tecante A., Gimeno M., Parra R., Garcia-Arrazola R. (2016). Removal strategies for endocrine disrupting chemicals using cellulose-based materials as adsorbents: A review. *Journal of Environmental Chemical Engineering*, 4(3), 3122-3142. https://doi.org/10.1016/j.jece.2016.06.025.

Tsamo C., Paltahe A., Fotio D., Vincent T.A., Sales W. F. (2019). One-, two-, and three-parameter isotherms, kinetics, and thermodynamic evaluation of Co (II) removal from aqueous solution using dead neem leaves. *International Journal of Chemical Engineering*, 2019, 1-14. https://doi.org/10.1155/2019/6452672.

Turp S.M., Turp G.A., Ekinci N., Özdemir S. (2020). Enhanced adsorption of methylene blue from textile wastewater by using natural and artificial zeolite. *Water Science and Technology*, 82(3), 513-523. https://doi.org/10.2166/wst.2020.358.

Unuabonah E.I., Omorogie M.O., Oladoja N.A. (2019). Modeling in adsorption: Fundamentals and applications. *In Composite nanoadsorbent,* 85-118. https://doi.org/10.1016/B978-0-12-814132-8.00005-8.

Wang H., Shadman, F. (2013). Effect of particle size on the adsorption and desorption properties of oxide nanoparticles. *AIChE Journal*, 59(5), 1502-1510. https://doi.org/10.1002/aic.13936.

Wulandary S. (2019). Sintesis Aerogel Selulosa dari Serat Batang Jagung dan Aplikasinya dalam Absorpsi Zat Warna Rhodamin B dan Metilen Biru.

Xia J., Gao Y., Yu G. (2021). Tetracycline removal from aqueous solution using zirconium-based metal-organic frameworks (Zr-MOFs) with different pore size and topology: Adsorption isotherm, kinetic and mechanism studies. *Journal of Colloid and Interface Science*, 590, 495-505. https://doi.org/10.1016/j.jcis.2021.01.046.

Yagub M.T., Sen T.K., Afroze S., Ang H.M. (2014). Dye and its removal from aqueous solution by adsorption: A review. *Advances in Colloid and Interface Science*, 209, 172-184. https://doi.org/10.1016/j.jcis.2021.01.046.

Zhang W., Pan Y.G., Huang W., Chen H., Yang H. (2019). Optimized ultrasonic-assisted extraction of papaya seed oil from Hainan/Eksotika variety. *Food Science & Nutrition*, 7(8), 2692-2701. https://doi.org/10.1002/fsn3.1125.

Zhang X., Gu, P., Liu Y. (2019). Decontamination of radioactive wastewater: State of the art and challenges forward. *Chemosphere*, 215, 543-553. doi.org/10.1016/j.chemosphere.2018.10.029.

(2023) ; https://revues.imist.ma/index.php/morjchem/index